Analysis of the SERS Spectrum by Theoretical Methodology: Evaluating a Classical Dipole Model and the Detuning of the Excitation Frequency

ARTICLE *in* THE JOURNAL OF PHYSICAL CHEMISTRY A · MAY 2013

Impact Factor: 2.69 · DOI: 10.1021/jp402926w · Source: PubMed

3 AUTHORS, INCLUDING:

Luca Guerrini
Medcom Advance SA
43 PUBLICATIONS **755** CITATIONS
SEE PROFILE

Ramón A Alvarez-Puebla
Catalan Institution for Research and Advance…
141 PUBLICATIONS **5,098** CITATIONS
SEE PROFILE

THE JOURNAL OF PHYSICAL CHEMISTRY A

Article

pubs.acs.org/JPCA

Analysis of the SERS Spectrum by Theoretical Methodology: Evaluating a Classical Dipole Model and the Detuning of the Excitation Frequency

Jose M. Hermida-Ramon,*[,†] Luca Guerrini,[†,‡,§] and Ramon A. Alvarez-Puebla*[,‡,§,∥]

[†]Departamento de Química-Física, Universidade de Vigo, 36310 Vigo, Spain

[‡]Departmento de Ingenieria Electronica, Universitat Rovira i Virgili, Avda. Països Catalans 26, 43007 Tarragona, Spain

[§]Centro de Tecnologia Quimica de Cataluña, Carrer de Marcel·lí Domingo s/n, 43007 Tarragona, Spain

[∥]Catalan Institution for Research and Advanced Studies (ICREA), Passeig Lluís Companys 23, 08010 Barcelona, Spain

Supporting Information

ABSTRACT: Surface-enhanced Raman scattering (SERS) spectroscopy is gaining prominence as one of the most powerful ultradetection techniques. The SERS outcome is essentially a complicated pattern of vibrational bands that allows multiplex analysis but, at the same time, makes difficult the interpretation of unknown analytes or known substances in the presence of complex unknown chemical environments. Herein, we show two computational methods to reproduce the spectral shape of the SERS spectra. The first, based in the modification of the classical dipole model, reproduces with a notable similarity the experimental spectrum excited far to the red of the localized surface plasmon resonance (LSPR). This light and time-efficient model is of great interest to elucidate the orientation of the target on the plasmonic surface or even to accurately identify suspected unknown targets in real samples. However, the experimental SERS spectrum in resonance with the LSPR is also modeled by using a more classical CPHF approach. This method provides also good agreement with the experiment but at the expense of much more computational time.

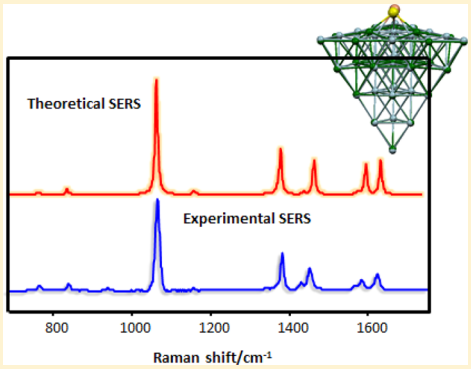

INTRODUCTION

Surface-enhanced Raman scattering (SERS) spectroscopy is evolving as one of the most powerful tools for analytical ultradetection.[1] SERS provides the characteristic vibrational signature of minute concentrations of analytes under their environmental conditions. Besides its straightforward application in the quantitative or semiquantitative identification of known analytes, many other fields are taking advantage of the unprecedented possibilities of this surface spectroscopy. For example, the sensitivity of SERS toward subtle changes[2] in the conformation or functionalization of the molecular target makes the technique appropriate for gaining information of biological systems, including *in vivo* cellular or intracellular reactions,[3,4] reaction mechanisms in catalysis,[5] or even to remotely analyze interesting components in unknown samples.[6] However, the advantage of offering such complex spectroscopic output (i.e., the characteristic vibrational pattern of the analyte), may turn into a disadvantage when dealing with unknown materials and/or molecular processes that alter the chemical or conformational structure of the analyte. If it is true that the molecular structure of an unknown substance can be elucidated from its vibrational fingerprint, this process is time-consuming and may imply a considerable extra experimental work.

To help with this task, theoretical calculations can drastically reduce time and effort.[7,8] Vibrational calculations at the *ab initio* level are, in fact, a mature field in classical spectroscopy (i.e., IR and Raman) yielding most of the times accurate assignments for all the vibrational modes of the molecular entity under study. In the case of SERS, however, these calculations are complicated because of the presence of the optical enhancer (i.e., the nanostructured plasmonic particle) and the active role that this extra element plays in determining the vibrational signature of the adsorbed molecule. Among the nanostructure-related effects, two major mechanisms contribute to SERS: the electromagnetic mechanism (EM) and the chemical mechanism (CM), which in turn can be separated into two different contributions, a nonresonant chemical mechanism (CHEM) and a charge-transfer mechanism (CT).[7] The EM effects result from the excitation of the localized surface plasmon resonances (LSPRs) induced by the incident light on the plasmonic enhancer (i.e., the EM effects are independent of the nature of the molecule) and, usually, are largely responsible for the SERS enhancements.[9] Theoretical studies of the electric field enhancements occurring on an ample variety of plasmonic

Received: March 25, 2013
Revised: May 10, 2013
Published: May 14, 2013

dx.doi.org/10.1021/jp402926w | J. Phys. Chem. A 2013, 117, 4584−4590

structures have been successfully carried out, in particular with the leading effort of the Schatz group,[7,8,10−13] by using classical electrodynamics methods, such as Mie theory, discrete dipole approximation (DDA), and finite difference time domain (FDTD). Nowadays, the modeling of the electromagnetic effects on the SERS spectra is a relatively established field of study. Differently, debate still remains on the exact contribution of the chemical mechanisms, which arise from the close chemical association between the molecule and the optical enhancer, to the overall SERS enhancement and the final spectral shape.[8,14−18] Several theoretical studies were performed to unravel the role played by chemical effects. Importantly, in recent studies by Neaton and co-workers[19,20] and by Jensen and co-workers,[21,22] density functional theory (DFT) and time-domain density functional theory (TDDFT) methods were exploited as efficient tools to elucidate the role of CHEM and CT mechanisms in shaping the SERS spectra of different adsorbates. Additionally, TDDFT methods proved to be successful in modeling the resonance Raman spectrum.[23] TDDFT methods are, nevertheless, highly time-consuming.

We here present two approaches based either in the modification of a classical (dipole) model[8,24] or in a coupled perturbed Hartee-Fock (CPHF)[12,25,26] method in order to reproduce the SERS spectrum profile under different illumination. Reproducibility of the spectral shape is the key element to identify unknown analytes but also the chemical changes or conformational dynamics of known molecules at the metal interface under different conditions.

EXPERIMENTAL MATERIALS AND METHODS

Chemicals. All chemicals were purchased from Aldrich-Fluka and used without further purification. Milli-Q water was used for all the experiments.

Silver Nanoparticle Synthesis. Citrate stabilized Ag colloids of ∼40 nm in diameter were prepared via seeded growth method.[27] First, seed gold nanoparticles of ca. 15 nm in diameter were synthesized following a modified Turkevich/Frens method.[28,29] $HAuCl_4$ trihydrate (25.4 μmol) was dissolved in 100 mL of milli-Q water and heated to boiling before the addition of 3 mL of a 1% w/w aqueous solution of trisodium citrate under vigorous stirring. The mixture was kept 30 min under reflux and then let to cool down at room temperature. In the second step of the seeded growth synthesis, 40 μmol of $AgNO_3$ were dissolved in 125 mL of milli-Q water and heated to boiling before adding, under vigorous stirring and in the following order, 8 mL of the gold colloids and 640 μL of a 1% w/w aqueous solution of trisodium citrate. After 30 min of reflux, an additional 4.9 mL of the 1% w/w aqueous trisodium citrate solution were added to the mixture, which was then further refluxed for 1 h.

Characterization. UV−vis−NIR spectra were recorded using an Agilent 8453 diode array spectrophotometer. TEM images were obtained using a JEOL JEM 1010 transmission electron microscope operating at an acceleration voltage of 100 kV.

Raman/SERS Spectroscopy. Raman and SERS experiments were conducted in a micro-Renishaw InVia Reflex system. The spectrograph uses high resolution gratings (1800 and 1200 grooves cm^{-1} for the visible and NIR, respectively) with additional band-pass filter optics. Excitation was carried out using laser lines at 442 and 830 nm. Average SERS of colloidal dispersions was carried out in 1 mL of as-prepared particle solutions with an analyte (2-naphthalenethiol) concentration of 10^{-6} M. Measurements were made by using a macrosampler accessory with integration times of 10 s and a power at the sample of 80 mW.

THEORETICAL METHODS

All quantum chemical calculations presented in this work were carried out using the density functional theory (DFT) methods by using Gaussian09 package.[30] Calculations were performed using the B3LYP (Becke, three-parameter, Lee−Yang−Parr) exchange-correlation functional[31] with a 6-31G* basis set to describe the 2-naphthalenethiol and a LANL2DZ relativistic effective core potential together with the corresponding basis set to describe the silver atoms.

Raman intensities are presented as the differential Raman scattering cross-section obtained from Raman scattering factors. Using the harmonic approximation, the differential Raman scattering is given by:[32−34]

$$\left(\frac{d\sigma}{d\Omega}\right)_i = \frac{(2\pi)^4}{45}(\bar{\upsilon}_0 - \bar{\upsilon}_i)\frac{h}{8\pi^2 c\bar{\upsilon}_i}\frac{1}{\left[1 - \exp\left(\frac{-hc\bar{\upsilon}_i}{k_B T}\right)\right]}S_i \quad (1)$$

where h, c, and k_B are the Planck constant, light speed, and Boltzmann constant, respectively; T is the temperature in Kelvin; $\bar{\upsilon}_0$ and $\bar{\upsilon}_i$ are the frequency of the incident light and of the ith vibrational mode, respectively; and, S_i is the Raman scattering factor for the i vibrational mode. S_i can be expressed as:

$$S_i = 45\left(\frac{d\alpha}{dQ_i}\right)^2 + 7\left(\frac{d\gamma}{dQ_i}\right)^2 \quad (2)$$

where $d\alpha/dQ_i$ and $d\gamma/dQ_i$ are the isotropic and anisotropic polarizability derivatives with respect to the vibrational mode i, respectively.

Quantum chemical calculations were carried out to obtain the nonfrequency-dependent Raman scattering factors that will provide the static Raman intensities. These intensities give an idea of the nonresonant chemical enhancements arising during molecule adsorption onto the metal cluster. In order to increase the agreement between the obtained results and the experimental SERS spectrum, we used two different approaches. The first, a modification of a classical (dipole) model,[7,8,24] estimates the Raman enhancement in SERS spectroscopy due to the strong local field. For this purpose, we considered the axis between the molecule and the nanoparticle. In a classical model, the parallel and perpendicular (to the axis) components of the local field at the molecule position can be approximated as:

$$E_{\parallel}^{loc} = 1 + \frac{2}{r^3}\alpha_{NP} \quad E_{\perp}^{loc} = 1 - \frac{1}{r^3}\alpha_{NP} \quad (3)$$

where r is the distance between the molecule and the nanoparticle, and α_{NP} is the polarizability of the nanoparticle. The parallel and perpendicular components of the Raman intensity considering the enhancement due to the field are then given by:

$$I_{\parallel}^{R} = I_{molecule}^{R}|E_{\parallel}^{loc}|^4 \quad I_{\perp}^{R} = I_{molecule}^{R}|E_{\perp}^{loc}|^4 \quad (4)$$

where $I_{molecule}^{R}$ is the Raman intensity of the isolated molecule. The vibration center for each normal mode is calculated through:

dx.doi.org/10.1021/jp402926w | J. Phys. Chem. A 2013, 117, 4584−4590

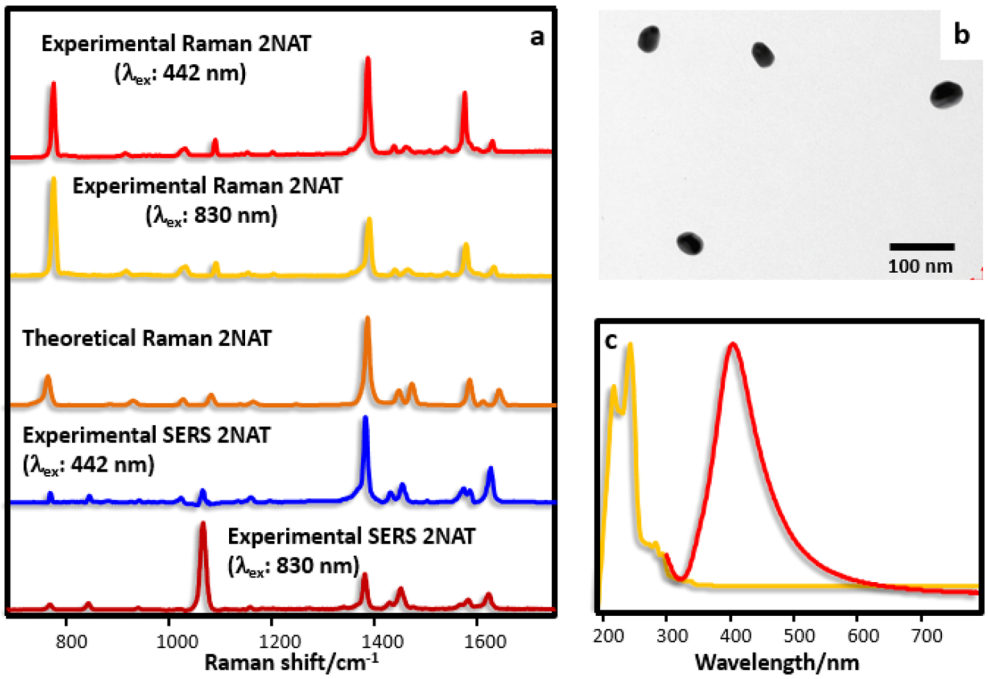

Figure 1. (a) Experimental and theoretical Raman spectra of bulk 2NAT; experimental SERS spectra of 2NAT on (b) colloidal silver particles, as excited with blue (442 nm) and NIR (830 nm) laser lines. (c) Electronic absorption of 2NAT (orange line) and LSPR of the silver nanoparticles (red line). Theoretical spectrum was obtained using DFT methods at the B3LYP/6-31G* level of theory and scaled at 0.9674.

$$C_i^{\mathrm{Nmode}} = \sum_{j=1}^{\mathrm{Natoms}} |\Delta_j^{\mathrm{Nmode}}| C_{i,j} / \sum_{j=1}^{\mathrm{Natoms}} |\Delta_j^{\mathrm{Nmode}}| \tag{5}$$

where $i = x, y, z$, C_i^{Nmode} are the different coordinates of the vibration center for a normal mode; $C_{i,j}$ are the coordinates of atom j, and $|\Delta_j^{\mathrm{NMode}}|$ is the module of the displacement for atom j in a given normal mode. For each normal mode, r is calculated in the eq 3 as the distance between the center of the nanoparticle and the vibration center. In order to obtain the enhancement due to the two components of the local field for each vibration, the angle between the vector of the atomic displacements and the axis perpendicular to the surface of the nanoparticle is calculated. Then the vector is split into the parallel and perpendicular components to this axis. By adding up all these atomic contributions, the parallel and perpendicular components for a normal mode are obtained (eqs 6 and 7).

$$\sum_{j=1}^{\mathrm{Natoms}} ((\cos^2 \alpha)_j + (\sin^2 \alpha)_j) |\Delta_j| / \sum_{j=1}^{\mathrm{Natoms}} |\Delta_j| = 1 \tag{6}$$

$$1 = \sum_{j=1}^{\mathrm{Natoms}} (\cos^2 \alpha)_j |\Delta_j| / \sum_{j=1}^{\mathrm{Natoms}} |\Delta_j| + \sum_{j=1}^{\mathrm{Natoms}} (\sin^2 \alpha)_j |\Delta_j| / \sum_{j=1}^{\mathrm{Natoms}} |\Delta_j| = W_{\parallel} + W_{\perp} \tag{7}$$

The enhancement due to each component (eqs 3) is multiplied by the value of the component and by the Raman intensity of the vibrational modes of the molecule attached to the cluster. We use the Raman intensity of the molecule in the cluster instead of the isolated molecule in order to take into account the chemical effects in the Raman spectrum. Finally, the total Raman intensity is the module of the vector formed by the two components; thus:

$$I_{\parallel}^{\mathrm{R}} = I_{\mathrm{cluster}}^{\mathrm{R}} W_{\parallel} |E_{\parallel}^{\mathrm{loc}}|^4 \quad I_{\perp}^{\mathrm{R}} = I_{\mathrm{cluster}}^{\mathrm{R}} W_{\perp} |E_{\perp}^{\mathrm{loc}}|^4$$
$$(I^{\mathrm{R}})^2 = (I_{\parallel}^{\mathrm{R}})^2 + (I_{\perp}^{\mathrm{R}})^2 \tag{8}$$

where W denotes the perpendicular and parallel components to the axis normal to the silver cluster surface.

The second approach relies on the use of a coupled perturbed Hartee−Fock (CPHF) method[12,2526] to obtain the frequency-dependent Raman scattering factors. In order to know the excitation frequency to calculate the frequency-dependent properties, a time-dependent DFT (TDDFT) calculation is performed in the complex formed by the molecule and the silver cluster. This calculation provides the electronic excitation frequency employed as the value of the frequency-dependent electric field that will be used in the calculations to represent the plasmonic effect in SERS.[8,12] However, during this process, the frequency-dependent properties become divergent for an electric field with a frequency in resonance with an electronic excitation frequency.[25,26,32] Nevertheless, Norman and Bishop[11] have shown that, by using a detuning of the excitation frequency, frequency-dependent properties can be calculated with a good accuracy. Taking this into account, we employed a detuning of the excitation frequency to avoid the divergence occurring at frequencies close to resonance. In order to check the reliability of this approach, an analysis of the simulated Raman spectra regarding the size of the detuning has been performed.

RESULTS AND DISCUSSION

Calculations at the DFT level normally yield accurate results compared with the experimental spectra. Figure 1a shows an excellent agreement between the experimental and theoretical Raman spectra of 2-naphthalenethiol (2NAT), a well-known Raman probe.[35] In this case, the theory fits the relative intensity of the experimental bands almost perfectly. Unfortunately, this is not the case with the SERS spectra. The SERS spectra were

dx.doi.org/10.1021/jp402926w | J. Phys. Chem. A 2013, 117, 4584−4590

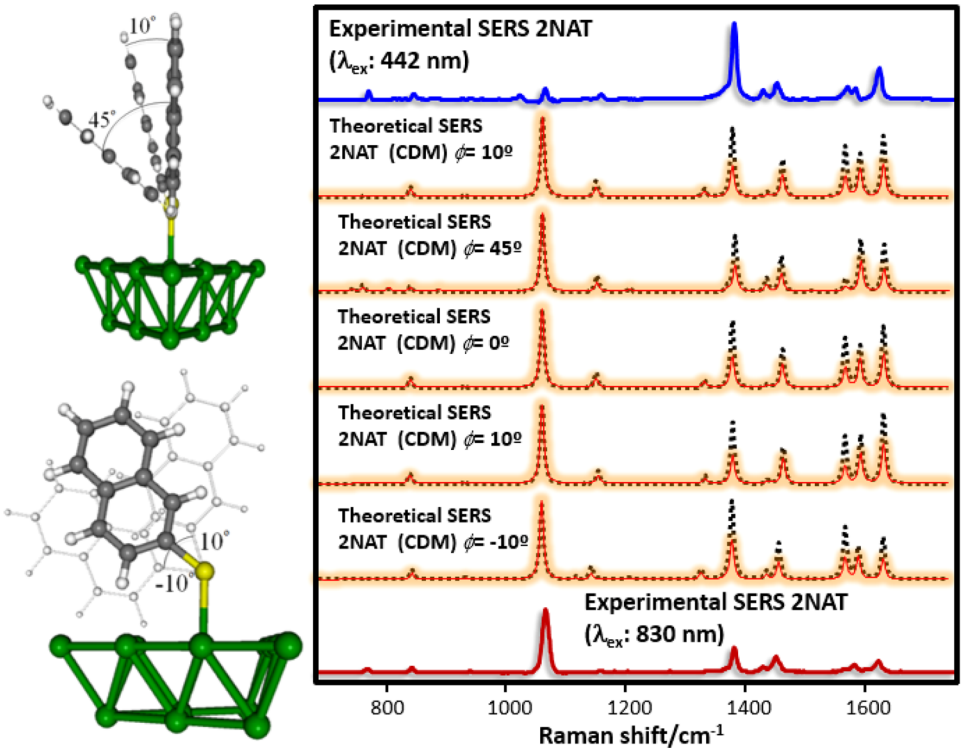

Figure 2. Theoretical model comprising the 2NAT chemically bound to a Ag_{16} cluster. Experimental SERS spectra of 2NAT excited with a blue or NIR laser. Theoretical Raman and SERS spectra of 2NAT varying the optimized orientation of the molecule on the cluster. The static Raman frequencies (dotted black spectra) were calculated by using B3LYP/6-31G* to describe the 2NAT. Silver was described with the LANL2DZ relativistic effective core potential together with the corresponding basis set. The SERS spectra (highlighted red lines) were calculated from the static frequencies by multiplying the intensity of each vibrational mode by a factor obtained applying a modified classical (dipole) model to estimate the electromagnetic enhancement in SERS spectroscopy due to the strong local field normal to the surface. All the theoretical spectra were scaled at 0.9674 (CDM, classical dipole model).

acquired by exciting the sample with two different laser lines, 442 and 830 nm, on silver spheroids of ∼40 nm diameters with a LSPR at 403 nm (Figure 1b,c). Both excitations are far away from the electronic absorption of 2NAT; thus, no chemical contributions from the analyte are expected. Notably, the SERS spectra differ markedly from both Raman spectra and between themselves (see, for example, the intensity ratio between the ring breathing at 1065 cm^{-1} and the ring stretching at 1380 cm^{-1}). In SERS the analyte is placed near a metallic surface that can be considered flat. Thus, besides the artifacts due to the quantum efficiency of the detector for different excitations,[36] which in this case are negligible due to the proximity of the two bands, two effects may be considered. First, the charge transfer effects induced by the light in the metal−analyte system that can be neglected for the 830 nm light but need to be considered when exciting at 442 nm. The second effect is due to the polarization of the local field (E^{loc}) at the surface, where the target molecule is placed. When using light far to the red of the bulk plasma resonance (830 nm), the perpendicular component of the surface dipole ($E_{\perp}^{loc}$) maximizes, increasing the intensity of the vibrational modes normal to the surface. Analogously, when the excitation is near the LSPR (442 nm), the parallel surface dipole ($E_{\parallel}^{loc}$) is significant.[37] As a consequence, the orientation of the molecule on the surface can be only safely inferred from the NIR excitation. This is corroborated in Figure 1a, where it is clear that the SERS spectrum excited with the blue laser is similar to the Raman, whereas the relative intensities of the bands are completely different in that excited in the NIR due to the impact of the surface selection rules.[37−39]

As a first approach to simulate the SERS spectra, a system comprising the analyte chemically bound to a fixed silver cluster of 16 atoms was built (Figure 2).[12] Quantum chemical calculations were carried out to obtain the nonfrequency-dependent Raman scattering factors that will provide the static Raman intensities. These intensities give an idea of the nonresonant chemical enhancements arising on a molecule adsorbed on a silver surface. The theoretical spectrum at the optimized geometry (ϕ = 0°) fits well the band position; however, it overestimates the intensity of the ring breathing at 1065 cm^{-1} in the case of the blue excitation. In the case of the NIR excitation, the model approaches better to the experimental profile; still, it overestimates the intensities of the ring stretchings between 1350 and 1600 cm^{-1}. As a result, the shape of optimized geometry (ϕ = 0°) in Figure 2 (highlighted red-line) greatly improves but still overestimates the ring stretchings. Bearing in mind the weight of the surface dipole in this calculation, the optimized geometry was forced to adopt different angles against the cluster surface. Notably, although still no geometry fully reproduces the experiment, a tendency toward the reduction of the intensity of the stretching modes was observed especially when the angle C−S−Ag was reduced by −10°.

This fact indicates that the lack of agreement is probably due to an improper orientation of the molecule on the surface. Considering that the molecular orientation may be influenced by the distortion of the first layer of silver atoms upon

dx.doi.org/10.1021/jp402926w | J. Phys. Chem. A 2013, 117, 4584−4590

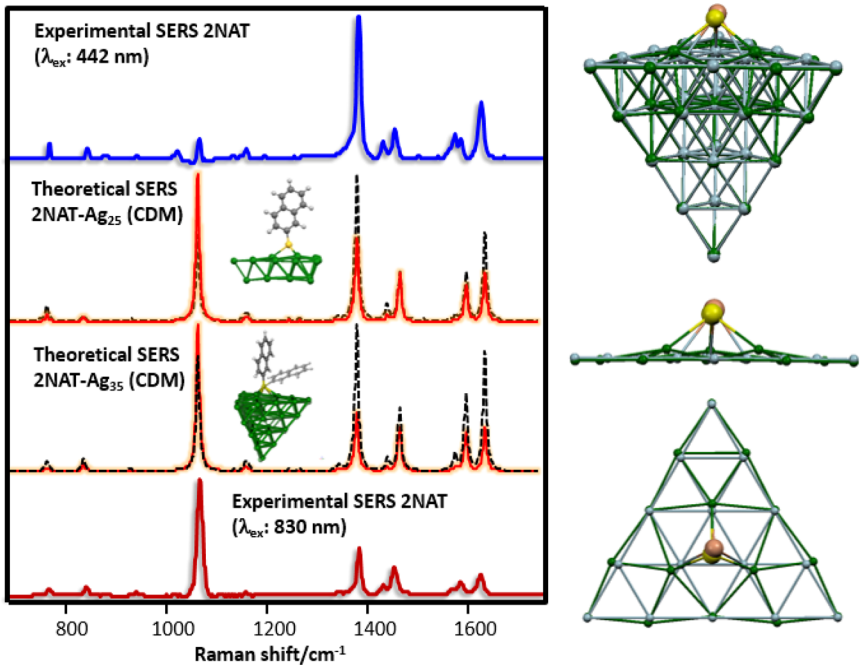

Figure 3. Experimental SERS spectra of 2NAT excited with a blue or NIR laser. Theoretical Raman (dotted-black lines) and SERS (highlighted red lines) spectra of 2NAT on the Ag_{25} or Ag_{35} cluster calculated using the modified classical dipole model. Different perspectives of the theoretical models before (Ag, gray, and S, orange) and after (Ag, green, and S, yellow) optimization (C and H are not shown). All the theoretical spectra were scaled at 0.9674 (CMD, classical dipole model).

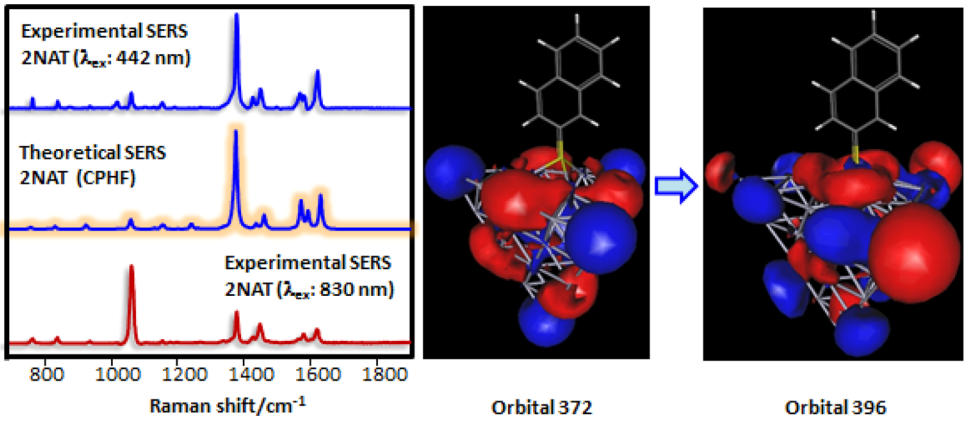

Figure 4. Experimental SERS spectra of 2NAT excited with a blue or NIR laser. Theoretical Raman spectrum of 2NAT on an Ag_{35} cluster (scaled at 0.9674) calculated using the CPHF method by exciting at 388 nm and its corresponding orbital transition.

interaction with the thiol,[40] we designed a new experiment on bigger clusters (Ag_{25} and Ag_{35})[41,42] where the geometry of the metal at the cluster was allowed to optimize as well. Figure 3 shows how after optimization the C−S−Ag angle slightly closes against the surface as a consequence of the redistribution of the first layer silver atoms. As a result, although both models notably improve the agreement with the SERS spectra excited in the NIR, those calculated in the bigger cluster reproduce almost perfectly the vibrational shape of the experiment. It is worthy of note that this method does not add extra time to the normal static calculations and subsequently can be performed regularly in a time efficient manner.

To calculate the experimental spectrum obtained by exciting with the blue laser, we employed a second approach that relies on the use of a coupled perturbed Hartee−Fock (CPHF) method[12,25,26] to obtain the frequency-dependent Raman scattering factors. To learn about the excitation frequency for the calculation of the frequency-dependent properties, a TDDFT calculation was performed in the 2NAT−Ag_{35} complex. During this process, the frequency-dependent properties become divergent for electric fields with values in resonance with the electronic excitation frequency.[8,26] To overcome this drawback, the excitation frequency was detuned.[26] The TDDFT calculation gave rise to several electronic transitions. Those with the largest oscillator strength are summarized in Table S1 (Supporting Information). Simulated spectra were obtained with all summarized electronic transitions and with some additional neighbor wavelengths, which are represented in Figure 4 and in the Supporting Information together with their corresponding orbital transitions. The CPHF calculated spectra offer extremely large values in their Raman activity but also large differences as a function of the excitation. This is due to the divergent behavior in wavelengths close to resonance. Since no damping factor[8] is

dx.doi.org/10.1021/jp402926w | J. Phys. Chem. A 2013, 117, 4584−4590

used in our calculations of the Raman intensity, at resonance wavelengths the Raman activity rises up to 10^{26}, while it decreases down to 10^{15} times for wavelengths 0.5 nm different; still, the shape of the spectrum is the same for the resonance and the neighboring wavelengths. Because of this fact, near-resonance Raman spectra are obtained, and the relative enhancement between the peaks is preserved when a detuning of the resonance frequency is performed. The orbital transition plots show the nature of the electronic transitions. There are transitions inside the silver cluster but also charge transfer transitions between the 2NAT and the cluster. As SERS is mainly due to the LSPR excitations,[8,33] in our model this corresponds to metal−metal excitations at 386.33 nm. To avoid the divergence within the resonance, the excitation was detuned to 388 nm, resulting in an extraordinary fit between the calculated and the experimental SERS at 442 nm (Figure 4). Unfortunately, in contrast with the previous model, the computational requirements for performing the CPHF calculations are considerably larger, resulting in computational times of several weeks.

CONCLUSIONS

In summary, herein we show two methods to reproduce the spectral shape of the SERS spectra. The first, based in the modification of the classical dipole model reproduces, with a notable similarity, the experimental spectrum excited far to the red of the LSPR. This light model is of great interest to elucidate the orientation of the target on the plasmonic surface or even to accurately identify suspected unknown targets in real samples. However, the experimental SERS spectrum in resonance with the LSPR is also modeled by using a more classical CPHF approach. This method provides also good agreement with the experiment but at the expense of much more computational time.

ASSOCIATED CONTENT

Supporting Information

Theoretical SERS spectra and orbital plots at different wavelength excitations. This material is available free of charge via the Internet at http://pubs.acs.org.

AUTHOR INFORMATION

Corresponding Author

*E-mail: jose_hermida@uvigo.es (J.M.H.-R.); ramon.alvarez@urv.cat (R.A.A.-P.).

Notes

The authors declare no competing financial interest.

ACKNOWLEDGMENTS

This work was funded by the Spanish Ministerio de Economia y Competitividad (CTQ2011-23167). J.M.H.-R thanks the Centro de Supercomputación de Galicia (CESGA) for access to computational facilities.

REFERENCES

(1) Sharma, B.; Frontiera, R. R.; Henry, A.-I.; Ringe, E.; Van Duyne, R. P. SERS: Materials, Applications, and the Future. *Mater. Today* **2012**, *15*, 16−25.

(2) Alvarez-Puebla, R. A.; Liz-Marzan, L. M. SERS Detection of Small Inorganic Molecules and Ions. *Angew. Chem., Int. Ed.* **2012**, *51*, 11214−11223.

(3) Lee, Y.-E. K.; Smith, R.; Kopelman, R. Nanoparticle PEBBLE Sensors in Live Cells and in Vivo. *Annu. Rev. Anal. Chem.* **2009**, *2*, 57−76.

(4) Ando, J.; Fujita, K.; Smith, N. I.; Kawata, S. Dynamic SERS Imaging of Cellular Transport Pathways with Endocytosed Gold Nanoparticles. *Nano Lett.* **2011**, *11*, 5344−5348.

(5) Kim, H.; Kosuda, K. M.; Van Duyne, R. P.; Stair, P. C. Resonance Raman and Surface- and Tip-Enhanced Raman Spectroscopy Methods to Study Solid Catalysts and Heterogeneous Catalytic Reactions. *Chem. Soc. Rev.* **2010**, *39*, 4820−4844.

(6) Lee, S. J.; Moskovits, M. Remote Sensing by Plasmonic Transport. *J. Am. Chem. Soc.* **2012**, *134*, 11384−11387.

(7) Morton, S. M.; Silverstein, D. W.; Jensen, L. Theoretical Studies of Plasmonics using Electronic Structure Methods. *Chem. Rev.* **2011**, *111*, 3962−3994.

(8) Jensen, L.; Aikens, C. M.; Schatz, G. C. Electronic Structure Methods for Studying Surface-Enhanced Raman Scattering. *Chem. Soc. Rev.* **2008**, *37*, 1061−1073.

(9) Stiles, P. L.; Dieringer, J. A.; Shah, N. C.; Van Duyne, R. R. Surface-Enhanced Raman Spectroscopy. In *Annual Review of Analytical Chemistry*; Annual Reviews: Palo Alto, 2008; Vol. *1*, pp 601−626.

(10) Chen, H.; McMahon, J. M.; Ratner, M. A.; Schatz, G. C. Classical Electrodynamics Coupled to Quantum Mechanics for Calculation of Molecular Optical Properties: A RT-TDDFT/FDTD Approach. *J. Phys. Chem. C* **2010**, *114*, 14384−14392.

(11) Schatz, G. C.; Young, M. A.; Van Duyne, R. P. *Electromagnetic Mechanism of SERS*; Kneipp, K.; Kneipp, H.; Moskovits, M., Eds.; Springer-Verlag: Berlin, Germany, 2006; Vol. *103*, pp 19-46.

(12) Zhao, L. L.; Jensen, L.; Schatz, G. C. Pyridine-Ag-20 Cluster: A Model System for Studying Surface-enhanced Raman Scattering. *J. Am. Chem. Soc.* **2006**, *128*, 2911−2919.

(13) Kleinman, S. L.; Sharma, B.; Blaber, M. G.; Henry, A. I.; Valley, N.; Freeman, R. G.; Natan, M. J.; Schatz, G. C.; Van Duyne, R. P. Structure Enhancement Factor Relationships in Single Gold Nanoantennas by Surface-Enhanced Raman Excitation Spectroscopy. *J. Am. Chem. Soc.* **2013**, *135*, 301−308.

(14) Lombardi, J. R.; Birke, R. L.; Lu, T. H.; Xu, J. Charge-Transfer Theory of Surface Enhanced Raman-Spectroscopy: Herzberg−Teller Contributions. *J. Chem. Phys.* **1986**, *84*, 4174−4180.

(15) Arenas, J. F.; Tocon, I. L.; Otero, J. C.; Marcos, J. I. Charge Transfer Processes in Surface-Enhanced Raman Scattering. Franck−Condon Active Vibrations of Pyridine. *J. Phys. Chem.* **1996**, *100*, 9254−9261.

(16) Persson, B. N. J.; Zhao, K.; Zhang, Z. Chemical Contribution to Surface-Enhanced Raman Scattering. *Phys. Rev. Lett.* **2006**, *96*.

(17) Lombardi, J. R.; Birke, R. L. A Unified View of Surface-Enhanced Raman Scattering. *Acc. Chem. Res.* **2009**, *42*, 734−742.

(18) Lombardi, J. R.; Birke, R. L. The Theory of Surface-Enhanced Raman Scattering. *J. Chem. Phys.* **2012**, *136*, 144704.

(19) Zayak, A. T.; Choo, H.; Hu, Y. S.; Gargas, D. J.; Cabrini, S.; Bokor, J.; Schuck, P. J.; Neaton, J. B. Harnessing Chemical Raman Enhancement for Understanding Organic Adsorbate Binding on Metal Surfaces. *J. Phys. Chem. Lett.* **2012**, *3*, 1357−1362.

(20) Zayak, A. T.; Hu, Y. S.; Choo, H.; Bokor, J.; Cabrini, S.; Schuck, P. J.; Neaton, J. B. Chemical Raman Enhancement of Organic Adsorbates on Metal Surfaces. *Phys. Rev. Lett.* **2011**, *106*, 083003.

(21) Moore, J. E.; Morton, S. M.; Jensen, L. Importance of Correctly Describing Charge-Transfer Excitations for Understanding the Chemical Effect in SERS. *J. Phys. Chem. Lett.* **2012**, *3*, 2470−2475.

(22) Morton, S. M.; Jensen, L. Understanding the Molecule-Surface Chemical Coupling in SERS. *J. Am. Chem. Soc.* **2009**, *131*, 4090−4098.

(23) Jensen, L.; Schatz, G. C. Resonance Raman Scattering of Rhodamine 6G as Calculated Using Time-Dependent Density Functional Theory. *J. Phys. Chem. A* **2006**, *110*, 5973−5977.

(24) Gersten, J.; Nitzan, A. Electromagnetic Theory of Enhanced Raman-Scattering by Molecules Adsorbed on Rough Surfaces. *J. Chem. Phys.* **1980**, *73*, 3023−3037.

(25) Wu, D. Y.; Zhao, L. B.; Liu, X. M.; Huang, R.; Huang, Y. F.; Ren, B.; Tian, Z. Q. Photon-Driven Charge Transfer and Photo-

catalysis of *p*-Aminothiophenol in Metal Nanogaps: a DFT Study of SERS. *Chem. Commun.* **2011**, *47*, 2520−2522.
(26) Norman, P.; Bishop, D. M.; Jensen, H. J. A.; Oddershede, J. Near-Resonant Absorption in the Time-Dependent Self-Consistent Field and Multiconfigurational Self-Consistent Field Approximations. *J. Chem. Phys.* **2001**, *115*, 10323−10334.
(27) Krpetic, Z.; Guerrini, L.; Larmour, I. A.; Reglinski, J.; Faulds, K.; Graham, D. Importance of Nanoparticle Size in Colorimetric and SERS-Based Multimodal Trace Detection of Ni(II) Ions with Functional Gold Nanoparticles. *Small* **2012**, *8*, 707−714.
(28) Turkevich, J.; Stevenson, P. C.; Hillier, J. A Study of the Nucleation and Growth Processes in the Synthesis of Colloidal Gold. *Discuss. Faraday Soc.* **1951**, 55−75.
(29) Frens, G. Controlled Nucleation for Regulation of Particle-Size in Monodisperse Gold Suspensions. *Nature [London], Phys. Sci.* **1973**, *241*, 20−22.
(30) Frisch, M. J.; Trucks, G. W.; Schlegel, H. B.; Scuseria, G. E.; Robb, M. A.; Cheeseman, J. R.; Scalmani, G.; Barone, V.; Mennucci, B.; Petersson, G. A.; et al. *Gaussian 09*, revision B.01; Gaussian, Inc.: Wallingford CT, 2009.
(31) Becke, A. D. Density-Functional Thermochemistry. III. The Role of Exact Exchange. *J. Chem. Phys.* **1993**, *98*, 5648−5652.
(32) Jensen, F. *Introduction to Computational Chemistry*; John Wiley & Sons: New York, 1999.
(33) Le Ru, E.; Etchegoin, P. *Principles of Surface Enhanced Raman Spectroscopy and Related Plasmonic Effects*; Elsevier: New York, 2009.
(34) Wu, D.-Y.; Liu, X.-M.; Duan, S.; Xu, X.; Ren, B.; Lin, S.-H.; Tian, Z.-Q. Chemical Enhancement Effects in SERS Spectra: A Quantum Chemical Study of Pyridine Interacting with Copper, Silver, Gold and Platinum Metals. *J. Phys. Chem. C* **2008**, *112*, 4195−4204.
(35) Alvarez-Puebla, R. A.; Dos Santos, D. S.; Aroca, R. F. SERS Detection of Environmental Pollutants in Humic Acid-Gold Nanoparticle Composite Materials. *Analyst* **2007**, *132*, 1210−1214.
(36) Alvarez-Puebla, R. A. Effects of the Excitation Wavelength on the SERS Spectrum. *J. Phys. Chem. Lett.* **2012**, *3*, 857−866.
(37) Moskovits, M.; Suh, J. S. Surface Selection-Rules for Surface-Enhanced Raman-Spectroscopy-Calculations and Application to the Surface-Enhanced Raman-Spectrum of Phthalazine on Silver. *J. Phys. Chem.* **1984**, *88*, 5526−5530.
(38) Moskovits, M.; Suh, J. S. The Geometry of Several Molecular Ions Adsorbed on the Surface of Colloidal Silver. *J. Phys. Chem.* **1984**, *88*, 1293−1298.
(39) Moskovits, M.; Suh, J. S. Surface Geometry Change in 2-Naphthoic Acid Adsorbed on Silver. *J. Phys. Chem.* **1988**, *92*, 6327−6329.
(40) Cossaro, A.; Mazzarello, R.; Rousseau, R.; Casalis, L.; Verdini, A.; Kohlmeyer, A.; Floreano, L.; Scandolo, S.; Morgante, A.; Klein, M. L.; et al. X-ray Diffraction and Computation Yield the Structure of Alkanethiols on Gold(111). *Science* **2008**, *321*, 943−946.
(41) Aikens, C. M.; Li, S.; Schatz, G. C. From Discrete Electronic States to Plasmons: TDDFT Optical Absorption Properties of Ag_n (n = 10, 20, 35, 56, 84, 120) Tetrahedral Clusters. *J. Phys. Chem. C* **2008**, *112*, 11272−11279.
(42) Jensen, L.; Zhao, L. L.; Schatz, G. C. Size-Dependence of the Enhanced Raman Scattering of Pyridine Adsorbed on Ag_n (n = 2−8, 20). *J. Phys. Chem. C* **2007**, *111*, 4756−4764.